17th Brazilian Congress of Thermal Sciences and Engineering
November 25th-28th, 2018, Águas de Lindóia, SP, Brazil

ENCIT-2018-0798
BEHAVIOR ANALYSIS SIMULATION OF SOLID PROPELLANT ROCKET ENGINE

George Stephane Queiroz de Oliveira
João Lucas Lobato Soares
Federal University of Pará- UFPA,FEM, Augusto Corrêa St., 1 - Guamá, Belém - PA, 66075-110
Georgeoliveira.ufpa@gmail.com
Soaresjoao974@gmail.com

Rene F. B. Gonçalves
Aeronautics Institute of Technology, Pç Mal Eduardo Gomes 50, São José dos Campos - SP, 12221-900
renefbg@ita.br

Abstract. *Propellant rocket motors presents higher efficiency and higher regression rate, when in comparison to liquid or hybrid motors, and also a storage of the charged motor. This work presents low-cost rocket engines, however the main objective is to fulfill all of the requirements of a rocket to be used in a space vehicle. Designing an engine requires a series of robust tools capable of understanding all the combinations of efforts in the operation of an engine, under high pressure and high temperature conditions. The detail of the process of designing a solid fuel rocket engine, from the initial hypotheses based on rocket engines with similar characteristics is shown.*

Keywords: *spacemodelism, rocket engines, CFD, Simulation analysis.*

1. INTRODUCTION

The variety of missions that a rocket can carry out is very large and ranges from small applications like attitude control of satellites to engines that drive the first steps of a launch vehicle. The mission of this rocket will be to raise a payload up to a certain height. Rocket motors are autonomous reaction motors, that is, they do not need ambient air for their operation. The propulsion is generated by the combustion of an existing mass in the vehicle, called propellant, which leaves the vehicle with a determined amount of associated movement. Therefore, the principle of conservation of the amount of movement, with this action increases the amount of movement of the vehicle in the opposite direction or is counteracted by aerodynamic and gravitational forces. The applications of this type of motors are fundamentally military, rockets air-ground and earth-ground for military missions, and some civil applications. In civil applications they are used, for example, in meteorological or scientific experimentation, such as for the measurement of radioactive components, or in grounding the results of telemetering in atmospheres contaminated by nuclear radiation.

According to the solid rocket motor is designed with the propellant inside the combustion chamber where it is simpler and easier for its handling and storage, however its disadvantage is that these have no control over its combustion after its ignition.

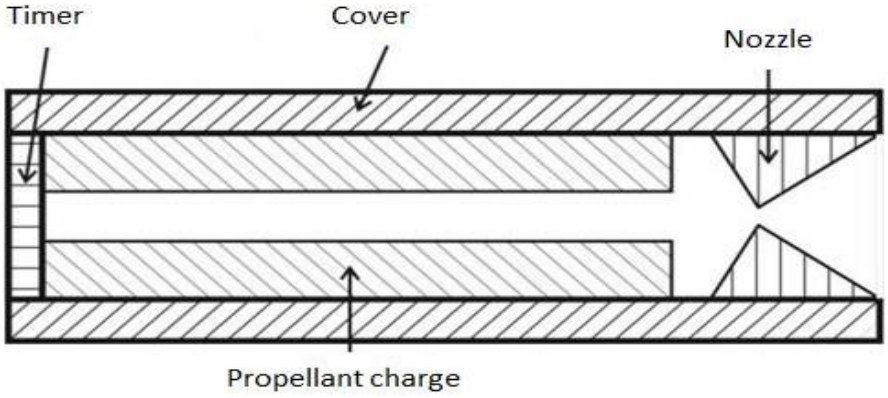

Figure 1: Scheme of a motor rocket.

The main object of the nozzle is to increase the pressure of the gases resulting from the burning of the propellant, in addition to increasing the escape velocity of the gases, thus raising the thrust of the engine. The timing cover or charge, depending on the case, is intended to prevent the gases from escaping from the side where it is placed If the timing load is chosen, a long firing time must be provided so that an ejector load can be ignited at the end of the load - which can eject the parachute or even the motor.

2. EXPERIMENTAL PROCEDURE

The computational analysis considered the viscous effects, the reactions of the chemical elements in the combustion process, their path over the motor and the nozzle and the values of the properties at each point within the geometry. Therefore, a mesh was created in reference to the design proposed by Taillandier, Marchi, Araki (2006).

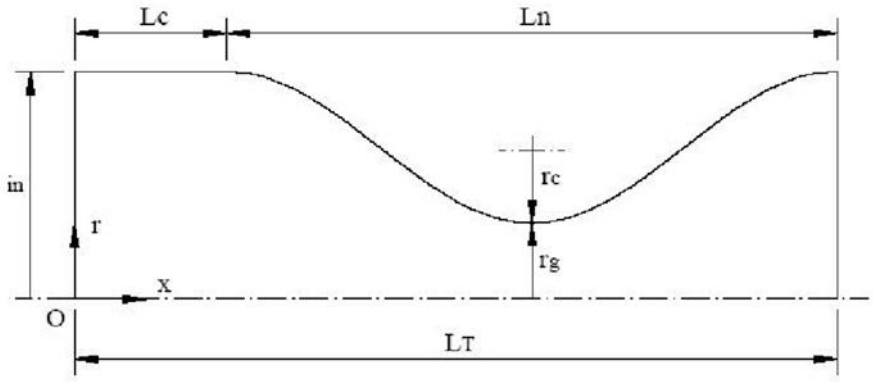

Figure 2: Geometry of the combustion chamber with the nozzle.

Thus, the geometry of the motor is defined, where:

Rg: Nozzle throat radius (Rg = 0.1m)
Rin: radius of the combustion chamber (Rin = 0.3m)
Rc: radius of curvature (Rc = 4.053x10-2m)
Lc: length of the combustion chamber (Lc = 0,1m)

the initial parameters of the solid propellant rocket motor, prior to the ignition where no changes in the system are possible, are room temperature (25 °C), ambient pressure (1 bar) and a one-dimensional flow.

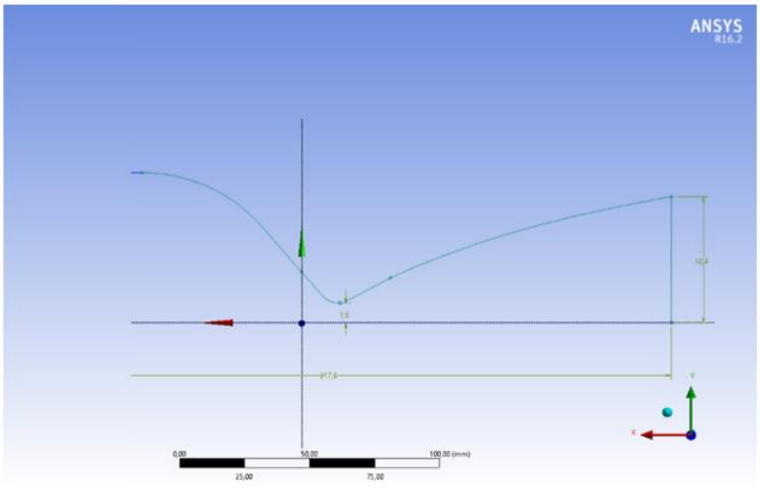

Figure 3: technical drawing of the combustion chamber with the nozzle.

A computational analysis of the rocket model to be used was carried out, considering the viscous effects, the reactions of the chemical elements in the combustion process, its routes over the motor and the nozzle, as well as the values of the properties in each point within the geometry.

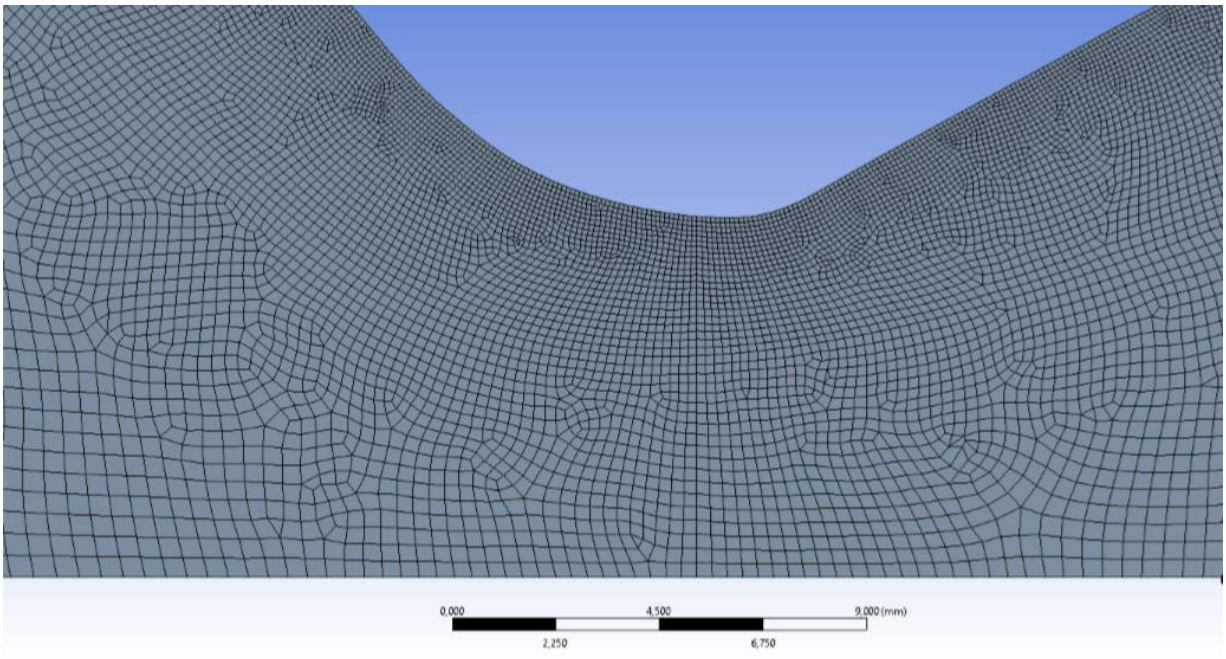

Figure 4: mesh refinement in the nozzle throat.

It was necessary to refine the mesh in the area of convergence-divergence in the nozzle throat so as to analyze the properties, and also to load a file of the reactive chemical elements in the software, to introduce the relaxation factors to the combustion solution. By attaching this file, the amount of each chemical element in the combustion reaction was considered. As a propellant, the material was chosen to be 35% of sucrose (sugar, $C_{12}H_{22}O_{11}$) and 65% of potassium nitrate (KNO_3), based on the literature., The form used of the grains was tubular, mainly for the ease of manufacture, since the matrices for this type of grain are simpler.

2.1 COMPUTATIONAL STUDY

The chemical elements were not previously mixed, the mixture occurs only inside the combustion chamber. The process of treatment of the energy was non-adiabatic, that is, the particles are free to exchange heat between them. The effects of the compressibility of the fluid were also considered. In addition, the diffusion behavior of the flame was treated as being stationary.

The k-ε turbulence models adopted have two equations that allow the determination of mixing length and time scale through the resolution of two different transport equations, which are present in ANSYS model k-ε, on which it has a base in transport equations for the kinetic energy of turbulence k and its dissipation rate ε, as presented below.

$$\frac{\partial}{\partial t}(\rho\kappa) + \frac{\partial}{\partial x_i}(\rho\kappa V_i) = \frac{\partial}{\partial x_j}\left[\left(\mu + \frac{\mu_t}{\sigma_\kappa}\right)\frac{\partial \kappa}{\partial x_j}\right] + G_k + G_b - \rho\varepsilon - Y_M + S_k \quad (1)$$

$$\frac{\partial}{\partial t}(\rho\varepsilon) + \frac{\partial}{\partial x_i}(\rho\varepsilon V_i) = \frac{\partial}{\partial x_j}\left[\left(\mu + \frac{\mu_t}{\sigma_\varepsilon}\right)\frac{\partial \varepsilon}{\partial x_j}\right] + C_{1\varepsilon}\frac{\varepsilon}{k}(G_k + C_{3\varepsilon}G_b) - C_{2\varepsilon}\rho\frac{\varepsilon^2}{k} + S_k \quad (2)$$

In these equations Gk represents the generation of turbulent kinetic energy due to the velocity gradients, Gb the generation of turbulent kinetic energy due to buoyancy, Ym represents the contribution of the floating expansion in compressible turbulent flow to the overall dissipation rate. The realizable K-ε model is also adopted for the work,

because it presents a better performance and thus can compare the obtained results, as well as mathematical modeling for transport equations for K and ε.

2.2 NUMERICAL STUDY

In the numerical study of the combustion of liquid fuel, is considered that some mathematical equations that describe the movement of particles in the reactive flow are the transport equation. ANSYS adopts the conservative form of the equations, considering that, within an infinitesimal control volume, the spatial variation is

$$\frac{\partial}{\partial t}\rho + \nabla.\rho\vec{V} = 0 \tag{3}$$

Therefore, for the fluid system properties to be conveyed continuously through a volume, can be described by the momentum equation, which was considered a Newtonian fluid, so the exact solution variables of the Navier-Stokes equation are decomposed into the mean components and floating.

$$V_i = \bar{V}_i + V'_i \tag{4}$$

The quantity of motion for compressible fluid equation adopted in this work is presented as

$$\frac{\partial}{\partial t}(\rho V_i) + \frac{\partial}{\partial x_j}(\rho V_i V_j) = -\frac{\partial p}{\partial x_i} + \frac{\partial}{\partial x_j}\left[\mu\left(\frac{\partial V_i}{\partial x_j} + \frac{\partial V_j}{\partial x_i} - \frac{2}{3}\delta_{ij}\frac{\partial V_l}{\partial x_l}\right)\right] + \frac{\partial}{\partial x_j}(-\rho\overline{V_i' V_j'}) \tag{5}$$

Thus, the left side of the equation represents the rate of change in the amount of movement that crosses the control surface per unit volume, the right side of the equation represents the external forces by volume units, which are the ones that act in the volume of control as the fluctuation generated by the turbulence.

To represent the temperature changes and eventual losses or heat gains representing the energy variation, as well as consumption and the production of species in the combustion process the transport equations of species and energy, are presented below.

$$\frac{\partial}{\partial t}(\rho Y_k) + \nabla.(\rho V Y_k) = -\nabla.(\rho Y_k V_k) + \dot{\omega}_k \tag{6}$$

3. RESULTS AND DISCUSSION

It is interesting to change the behavior of the properties over time during the combustion process inside the combustion chamber. By comparing the 3 time intervals, it is noted that the peak pressure decreases by about 1 bar every 4 seconds. The maximum temperature in the converging part of the nozzle also has its maximum value initially of 3150 K, and every 4 seconds it decreases around 200 K. With respect to the output density of the fluid, it increases a little over time, around 10^{-3}, the velocity of the sound has a behavior similar to temperature, because they are directly related. Finally, the velocity and the Mach number have maximum values initially, and gradually decrease with the passage of time.

The temperature and the velocity of the sound have a greater difference compared to the previous results, having an almost constant behavior in the divergent part of the nozzle. The variation of the Mach number is also not very large in this area. However, the decrease of the pressure and the exit velocity of the fluids have a similar behavior, a little superior compared to the viscous case.

Result when the time is t = 0s

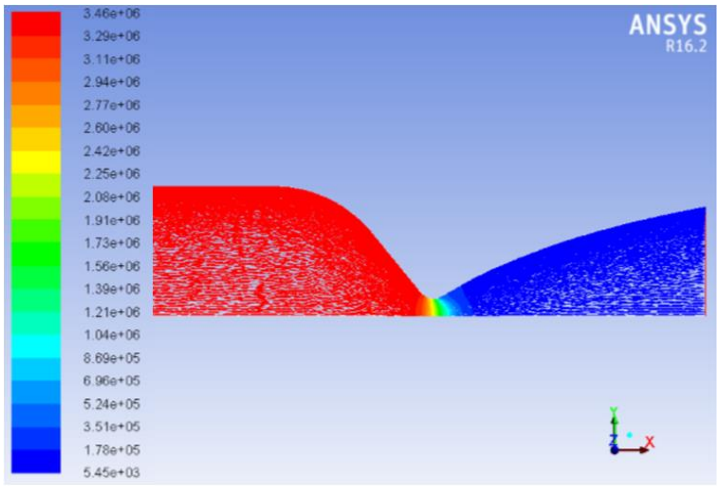

Figure 5 : Pressure distribution along full geometry.

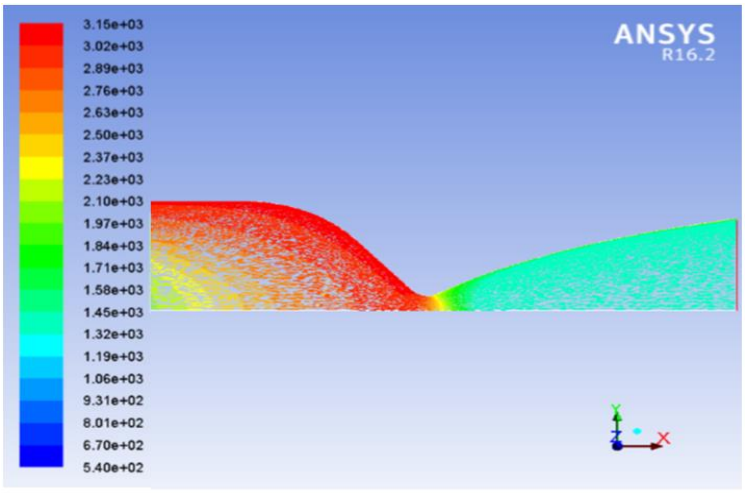

Figure 6 : Temperature distribution along the complete geometry.

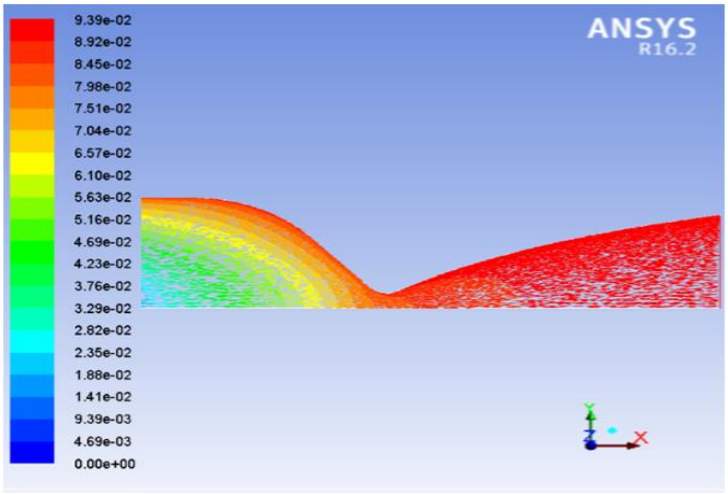

Figure 7: Distribution of water along full geometry.

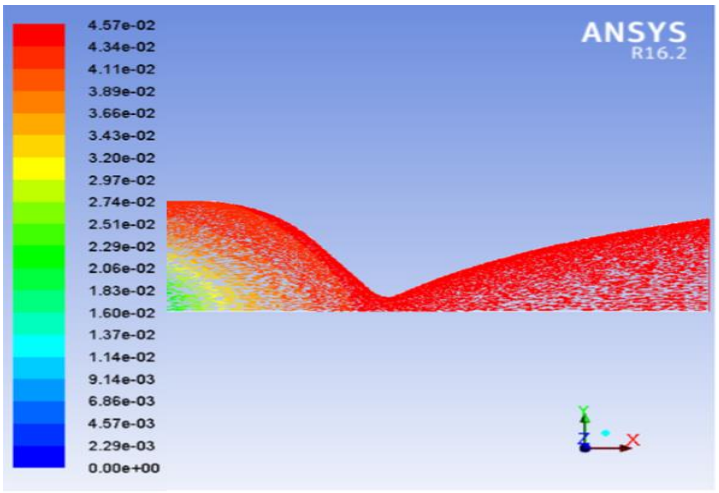

Figure 8 : Distribution of carbon dioxide along the complete geometry.

Result when the time is t=4s.

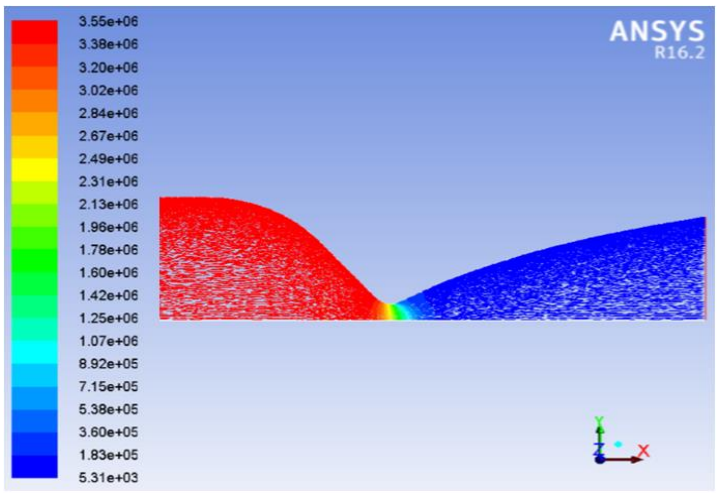

Figure 9 : Pressure distribution along full geometry.

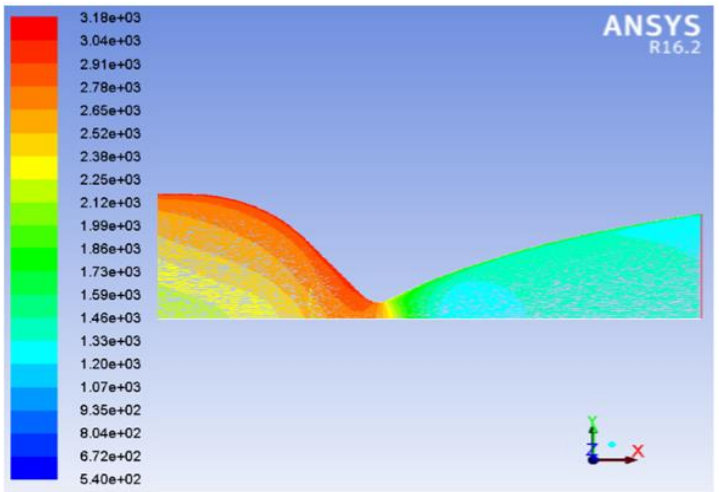

Figure 10 : Temperature distribution along the complete geometry.

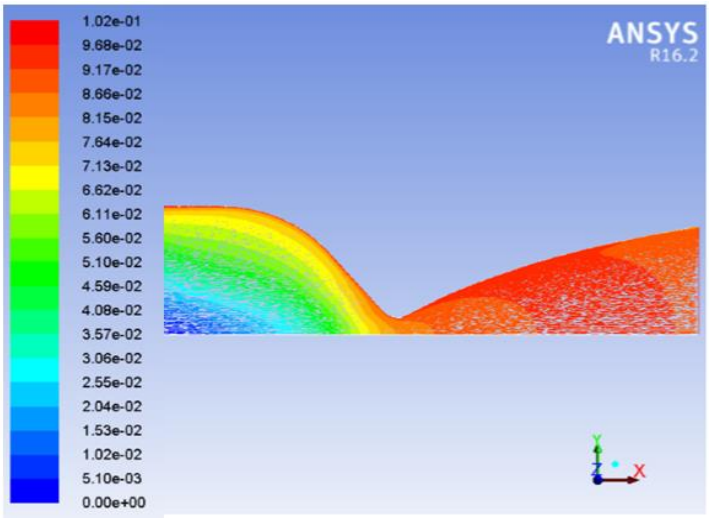

Figure 11: Distribution of water along full geometry.

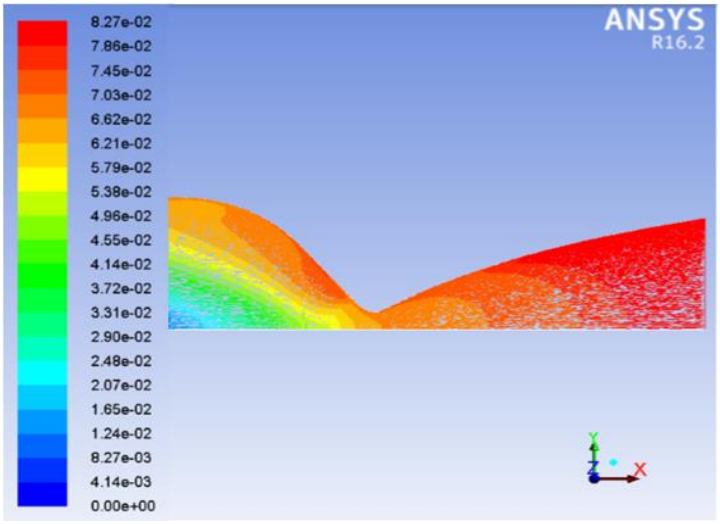

Figure 12 : Distribution of carbon dioxide along the complete geometry.

Result when the time is t=8s

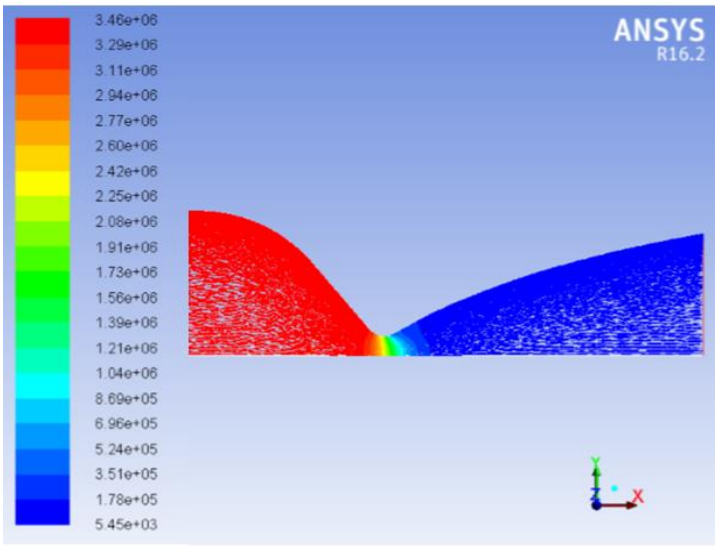

Figure 13 : Pressure distribution along full geometry.

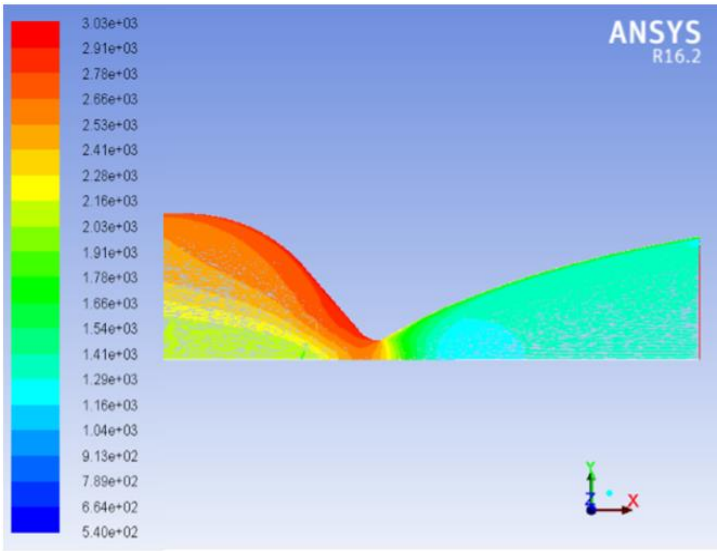

Figure 14: Temperature distribution along the complete geometry.

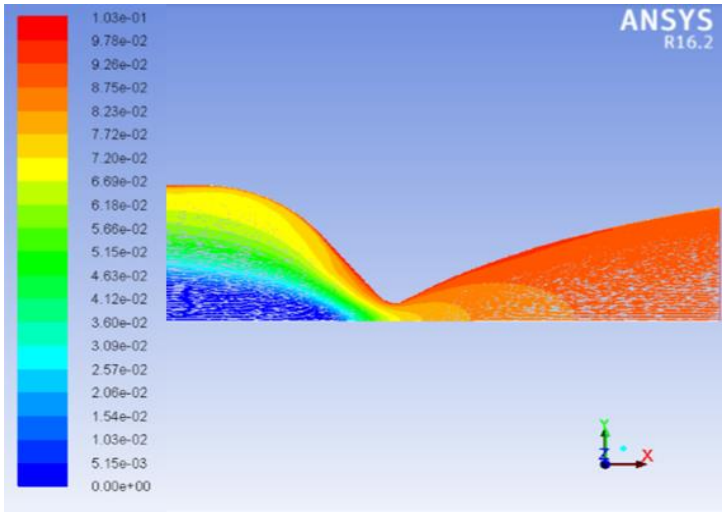

Figure 15: Distribution of water along full geometry.

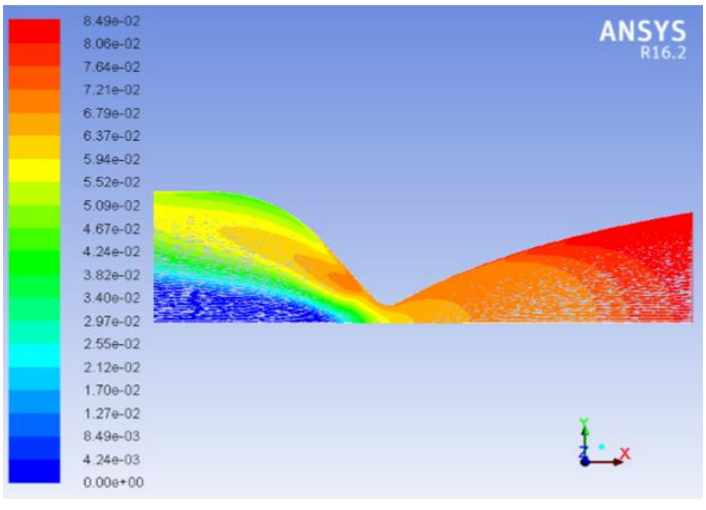

Figure 16 : Distribution of carbon dioxide along the complete geometry.

The variation of the values of the chemical elements is also very coherent along with the deliberate properties in the initial condition. The combustion products initially have the largest distribution at the exit of the nozzle and in the convergent part, over time that concentration decreases, which is explained by the decrease in the power of the combustion process, ie $C_{12}H_{22}O_{11} + KNO_3$, which is burned over time and has a burning time of only 8.5 seconds.

4. ACKNOWLEDGEMENTS

Thanks to the group PETMEC tutorial education program of Mechanical Engineering.

5. REFERENCES

SHYNKARENKO A. ANDRIANOV, A. B. O.; JR., M. N. D. B. Concept and design of the hybrid test-motor for the development of a propulsive decelerator of sara reentry capsule. 2015.

JR, J. D. A. Fundamentals of aerodynamics. [S.l.]: Tata McGraw-Hill Education, 2011.

SUTTON, G. P.; Rocket Propulsion Elements: An introduction to the enginneering of rockets", 2001. Peterson, P. H. C.; Mechanics And Thermodinamics of Propulsion, 2nd edition, 1992.

Weiss, W.; Sessler, J. G.; Aerospace Structural Metals Handbook, Vol. I, Syracuse Univerity, Research Center, 1963. Barrère, M.; Jaumotte, A.; Vandenkerckhove, J.; Rocket Propulsion, Elsevier Publishing Company, 2nd Edition, 1960. Gutheil, E. 2011. Issues in Computational Studies of Turbulent Spray Combustion. Experiments and Numerical

Simulations of Diluted Spray Turbulent Combustion. ERCOFTAC Series, vol 17. Spring, Dordrecht.

Foltran ,A. C. Moro, D .F, Silva N.D.P, Ferreira, A.E.G, Araki, L. K , Marchi, C. H, Burning Rate Measurement of KNSu Propellant Obtained by Mechanical Press, 2015

6. RESPONSIBILITY NOTICE

The author(s) is (are) the only responsible for the printed material included in this paper.